Investigations of crystallinity and residual stress of cubic boron nitride films by Raman spectroscopy

W. J. Zhang and S. Matsumoto
National Institute for Research in Inorganic Materials, 1-1 Namiki, Tsukuba, Ibaraki 305-0044, Japan
(Received 27 April 2000; revised manuscript received 5 September 2000; published 23 January 2001)

With a spatial correlation model, a simple method was established to evaluate the crystallinity and stress of cubic boron nitride (cBN) films from the variation of linewidth and peak shift of Raman spectra. An increase of crystallinity and a decrease of stress of the cBN films with growth time were demonstrated. As a reference, the Raman spectra of cBN single crystals synthesized by a high-pressure, high-temperature method were also investigated. Our cBN film deposited for 1 h revealed a low stress of about 1 GPa and a comparable crystallinity to that of 4–8 μm commercially available cBN single crystals.

DOI: 10.1103/PhysRevB.63.073201 PACS number(s): 78.30.−j, 61.10.Eq, 63.20.Dj, 81.15.Gh

Cubic boron nitride (cBN) films, which are expected to possess excellent physical and chemical properties comparable or superior to those of diamond films, have significant technological potential for applications for cutting tools and optical and electronic devices. Up to now, there have been many reports of the synthesis of cBN films by use of low-pressure physical[1–5] and chemical[6–9] vapor deposition. However, only multiple-phase boron nitride films with a nanocrystalline structure were achieved, and these films typically have a large internal stress caused by ion bombardment and therefore a limit of film thickness (tens to hundreds of nanometers) and poor adhesion with substrates. Characterization of BN films is nontrivial, and conclusive phase and crystallinity identification requires application of several complementary techniques including Fourier-transform infrared spectroscopy, electron and x-ray diffraction, transmission electron microscopy, electron energy-loss spectroscopy, and some other techniques.[10,11] Meanwhile, the evaluation of the residual stress is also complex due to the small film thickness and poor adhesion of the cBN films with substrates up to date. Raman analysis is much less affected by factors such as film thickness and the optical properties of the substrate, and it can simultaneously give information on phase composition, crystallinity, and even stress. However, it has been shown that the Raman peaks of cBN substantially broaden as the crystallite size decreases or the amount of defects increases.[6,12] This leads to difficulty in obtaining well-defined Raman spectra from current cBN films composed of only small, highly defective crystallites. Raman spectroscopy investigations have so far mainly been performed for single crystals by a high-pressure, high-temperature (HPHT) method.

Recently, thick cBN films were successfully prepared on Si substrates by dc jet plasma chemical vapor deposition (CVD) in an $Ar/N_2/BF_3/H_2$ gas system.[13] The deposition of such thick cBN films allows us to investigate the Raman spectra of cBN films deposited by CVD. By using a spatial correlation model, the crystallinity and residual stress of our cBN films and their dependence on the deposition time were revealed at the same time.

Figures 1(a) and 1(b) show the scanning electron microscopy (SEM) cross-sectional morphologies of cBN films deposited for 10 and 60 min, respectively. Columnar growth for both films can be clearly seen, and film thicknesses of about 3 and 12 μm were obtained for 10 and 60 min depositions. The corresponding Raman spectra of these two samples are shown in Fig. 2. For reference, the Raman spectra of HPHT cBN crystals of size 4–8 μm (commercially available from Showa-Denko) and 0.4 mm (from GE) are also given in Fig. 2. The laser power was kept below 50 mW for the Raman measurements to minimize the influence of temperature variation on the measurements. It can be seen that both transverse (TO) and longitudinal optical (LO) cBN modes appear strongly in the spectra. The peak position and full width at half maximum (FWHM) of each spectrum are summarized in Table I. For HPHT crystals, the peak position is downshifted and the peaks become asymmetrically broad as the crystal size decreases, which agrees well with previous

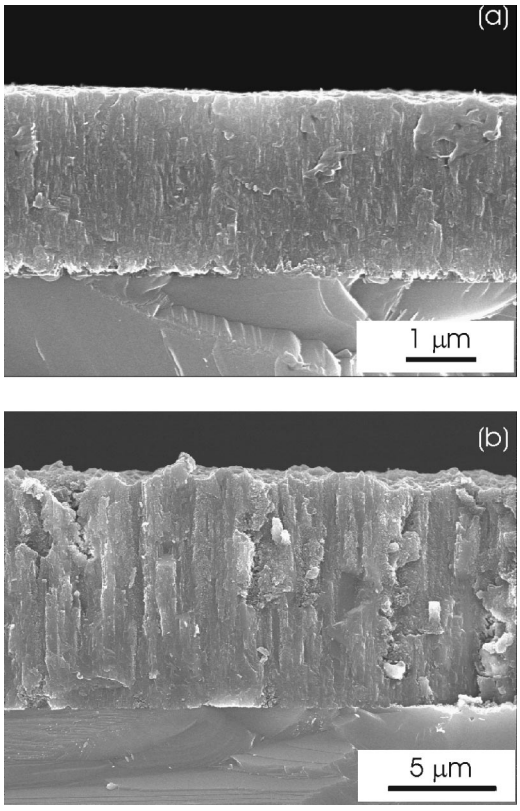

FIG. 1. SEM cross-sectional morphologies of cBN films deposited for (a) 10 and (b) 60 min.

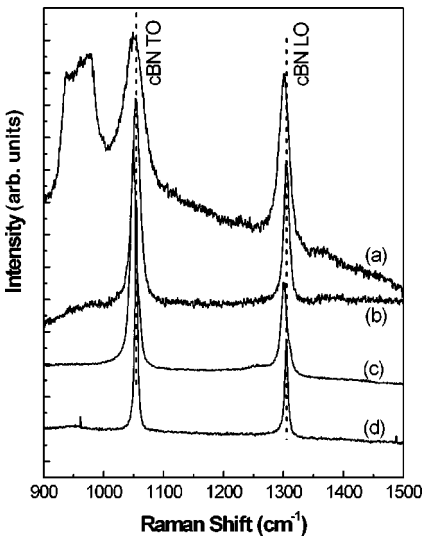

FIG. 2. Raman spectra of cBN films deposited for (a) 10 and (b) 60 min and (c) 4–8 μm and (d) 0.4 mm commercially available HPHT cBN crystallites.

results.[12] For the CVD films, a decrease of Raman linewidth was also observed as the growth time increased, but the variation of peak positions cannot simply be explained by only the size effects. It should be noticed that the cBN film deposited for 1 h shows a similar linewidth for both TO and LO modes, and therefore, as discussed below, has a comparable crystallinity to that of the 4–8 μm cBN single crystals. To our knowledge, this is the best crystallinity for cBN films deposited by either chemical or physical vapor deposition up to now.

The downshift and asymmetric broadening of Raman lines have been reported for microcrystalline Si and Ge,[14,15] semiconductor alloys,[16,17] and diamond.[18] Parayanthal and Pollak[16] have developed a spatial correlation model to explain such changes in the Raman spectra. Werninghaus *et al.*[12] used this model to investigate size effects of cBN crystals obtained by the HPHT method and as well as a cBN film obtained by PVD. However, only the LO mode was obtained in their cBN film and the peak intensity was actually too weak to have a satisfactory simulation. Moreover, a high residual stress typically exists in cBN films obtained by PVD due to the ion bombardment during deposition, which is known to cause a shift of the Raman peaks, and was not considered in their work.

TABLE I. Peak position and FWHM of TO and LO Raman modes of the spectra shown in Fig. 2.

Sample	Mode	Peak position (cm^{-1})	FWHM (cm^{-1})
CVD 10 min	TO	1048.4	28.8
	LO	1301.8	19.7
CVD 60 min	TO	1053.6	14.8
	LO	1304.8	10.4
HPHT 4–8 μm	TO	1049.6	12.5
	LO	1301.3	11.1
HPHT 0.4 mm	TO	1054.8	5.1
	LO	1304.8	7.2

The spatial correlation model is based upon the fact that, in an infinite crystal, only phonons near the center of the Brillouin zone ($q \approx 0$) contribute to the Raman spectrum because of momentum conservation between phonons and incident light. On the other hand, in a finite crystal, phonons can be confined in space by crystal boundaries or defects. This results in uncertainty in the phonon momentum, allowing phonons with $q \neq 0$ to contribute to the Raman spectrum.[14,16] As a result, the Raman line shape can be calculated by superimposing Lorentzian line shapes centered at $\omega(q)$, weighted by the wave-vector uncertainty caused by the confinement:

$$I(\omega) \cong \int_0^1 \frac{\exp(-q^2L^2/4)4\pi q^2 dq}{[\omega-\omega(q)]^2+(\Gamma_0/2)^2}. \quad (1)$$

Here $\omega(q)$ is an approximate one-dimensional phonon dispersion curve. q is expressed in units of $2\pi/a$ and the correlation length L is in units of a, with $a=3.6157$ Å being the lattice constant of cBN. Γ_0 is the natural linewidth ($\Gamma_0 = 3.5\,cm^{-1}$, measured in 0.8 mm single-crystalline cBN at room temperature, was used in our simulations).[18,19] For the phonon dispersion curve $\omega_{LO}(q)$ of the LO mode a theoretical calculation by Karch *et al.*[20] was used in this work, which can be polynomially fitted as[12]

$$\omega_{LO}(q) = 1284.2 - 0.1(q) - 147.94(q)^2 + 81.39(q)^3 + 726.79(q)^4 - 1870.13(q)^5 + 1074.72(q)^6. \quad (2)$$

From this equation, $\omega_{LO}(q)$ at the $\Gamma(q=0)$ point is calculated to be 1284.2 cm^{-1}. However, from experimental observations the Raman frequency at the Γ point is dependent on the temperature and 1305.4 cm^{-1} was obtained at room temperature.[19] Since the theoretical calculation of the dispersion curve has been shown to provide more accurate information on the curvature of $\omega(q)$ than on the absolute frequency,[12] we rigidly upshifted the dispersion curve by 21.2 cm^{-1} in this work.

Figure 3 shows the Raman line shapes of the cBN LO mode calculated with Eq. (1) at correlation lengths of 10, 20, 50, and 100 Å, respectively. It is clearly seen that the peak downshifted to lower wave number and became asymmetrically broadened as the correlation length decreased from 100 to 10 Å. By using the correlation length $L=35$ Å, the Raman LO mode of 4–8 μm HPHT crystallites can be well fitted, as shown in Fig. 4(a). For the cBN film deposited for 10 min, $L=20$ Å was used to fit the spectrum, shown as the dotted line in Fig. 4(b). A similar line shape as measured experimentally was obtained; however, the simulated peak position is 4.8 cm^{-1} lower than the experimental data. Considering that ion bombardment of the substrate was performed during the deposition process by applying a negative bias, compressive residual stress should exist in the film. It has been demonstrated that a compressive pressure of 1 GPa will cause the LO peak to upshift by 3.45 cm^{-1}.[21] Using this value (3.45 cm^{-1}/GPa) and assuming a compressive stress of -1.5 GPa in the film, a good fit can be achieved, as shown by the solid line in Fig. 4(b). Therefore, a compressive stress of -1.5 GPa in this film is suggested. Following the same route, the Raman LO mode of the cBN film deposited for 60

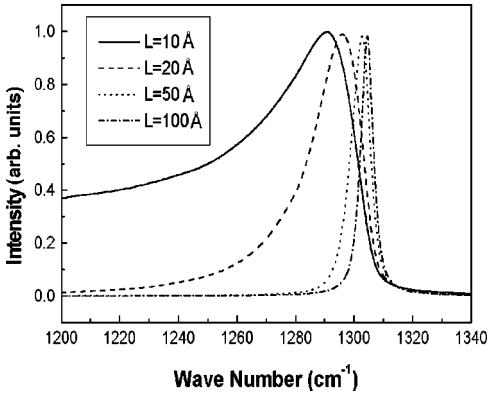

FIG. 3. Raman line shapes calculated with the spatial correlation model for different values of correlation length. $L=10$ Å, solid line; 20 Å, dashed line; 50 Å, dotted line; and 100 Å, dash-dotted line.

min can also be well fitted with $L=37$ Å and a compressive stress of 1.0 GPa, as shown in Fig. 4(c). The increase of correlation length of the sample deposited for 60 min demonstrates an improvement of the crystallinity, i.e., increase of crystal size and/or decrease of grain boundaries and defect states. Meanwhile, a decrease of stress with deposition time was revealed, which may be due to annealing effects by the high substrate temperature during deposition. The decrease of residual stress allowed us to deposit thick and adhesive cBN films of 12 μm and even more.

As shown in Table I, the TO modes of the spectra should undergo similar changes in both peak position and linewidth as the LO modes. To fit the TO mode, a phonon dispersion curve $\omega_{\mathrm{TO}}(q)$ can also be obtained from the calculations by Karch *et al.*[20] We tried to fit the TO modes following the same method as for the LO mode. However, even for the HPHT samples, the fits were not satisfactory. This is possibly because the calculated dispersion curve for the TO mode in Ref. 20 is not accurate.

To confirm the results from Raman measurements, glancing-angle x-ray diffraction (XRD) was carried out to investigate the crystal size and stress of our cBN films as shown in Fig. 5. The incident x-ray angle α was set at 0.05° and the diffraction pattern was taken in the 2θ continuous mode with a step width of 0.02°. The crystal size can be obtained from the diffraction patterns by using the well-known Sherrer equation:

$$L_{hkl}=\frac{K\lambda}{\sqrt{(B^2-b^2)}\cos\theta}. \tag{3}$$

Here $K=0.9$, $\lambda=1.5418$ Å, and B and b are the FWHM of the diffraction peak and instrumental broadening, respectively. Furthermore, the strain ϵ_{ψ} was calculated from the lattice distortion $(d_0-d)/d_0$, where d and d_0 are the lattice spacing of the measured cBN reflection and the corresponding value from JCPDS-35-1365, respectively. Assuming a biaxial stress and neglecting shear components in the film, the stress can be roughly estimated by using Hooke's law:

$$\sigma=\varepsilon_{\psi}E/(1-\gamma). \tag{4}$$

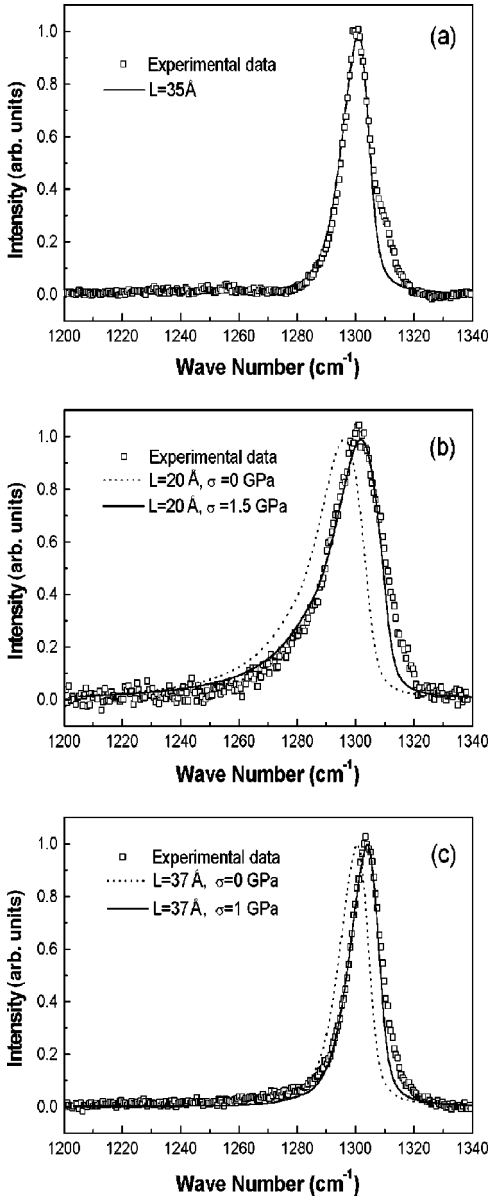

FIG. 4. Experimental data and line shapes calculated using spatial correlation model for the Raman LO mode of (a) 4–8 μm HPHT cBN crystallites ($L=35$ Å), and of cBN films deposited for (b) 10 ($L=20$ Å) and (c) 60 min ($L=37$ Å).

Here the Young's modulus of the cBN film $E=833$ GPa and the Poisson ratio $\gamma=0.112$.[22] To ensure precision, we used the strongest 111 peak for the calculation of crystal size, and used both 111 and the second strongest peak 220 for the calculation of stress. The calculated crystal sizes and stresses from glancing-angle XRD measurements, and the correlation length L and stress evaluated from Raman spectroscopy, are summarized in Table II. The agreement of the stress obtained by both methods shows that it is possible to evaluate the residual stress from simulations of Raman spectra using the spatial correlation model. It can be seen that the crystal size increased from about 180 to 270 Å as the deposition time increased from 10 to 60 min; correspondingly the correlation length increased from 20 to 37 Å. This coincides well with the results obtained from HPHT cBN crystallites that corre-

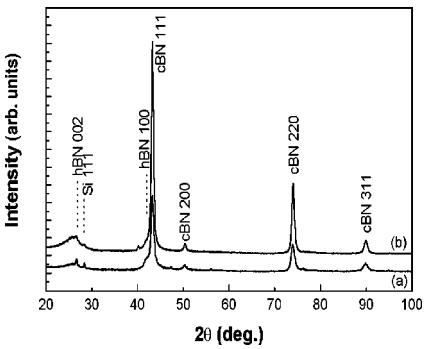

FIG. 5. Glancing-angle XRD patterns of the cBN films deposited for (a) 10 and (b) 60 min.

lation length increases with increase of crystal size.[12] It should be noted that the correlation lengths from our fittings are almost one order of magnitude smaller than the crystal sizes obtained from XRD measurements. However, in previous Raman studies of microcrystalline Si and GaAs,[14,17] it was observed that correlation length agreed with microcrystalline size. On the contrary, it was also found that the correlation length was smaller than the microcrystalline size in Raman fits of microcrystalline Si and Ge systems,[15] which was shown to be due to phonon confinement by impurities rather than by the grain boundaries. In our case, high-density defects including twins and stacking faults were observed in the crystals by transmission electron microscopy (TEM).[23] Although these defects and other kinds of defect, i.e., point defects and impurities that were not observed by TEM but should exist in the crystals, also lead to underestimation of the crystal size by XRD, an even smaller correlation length than the crystal size calculated from XRD is not surprising because of the different mechanism of defect-induced line broadening in Raman spectroscopy and XRD. Overall, the correlation length can be considered as an index representing the film quality that depends not only on the crystal size but also on the average mean free path of the electron-phonon system related to the defect density and/or impurities. Only when the crystal size is small (in the range of nanometers or micrometers) and/or the defect density and impurity content in the crystals are low enough do the grain boundaries dominate the phonon confinement process and then the correlation length can agree with the crystal size.

TABLE II. Comparison of the correlation length and stress obtained from simulation of Raman spectra of cBN films with the crystal size and stress calculated from glancing-angle XRD.

	Raman spectroscopy		X-ray diffraction	
Sample	Correlation length (Å)	Stress (GPa)	Crystal size (Å)	Stress (GPa)
CVD 10 min	20	−1.5	180	−1.3–−2.0
CVD 60 min	37	−1.0	270	−0.9–−1.9

In conclusion, Raman spectra of cBN films can be simulated with the spatial correlation model together with consideration of the effect of residual stress. Based on the simulation, an effective method was established to evaluate the crystallinity and stress of the cBN films from the variation of linewidth and peak shift of the Raman LO mode. This study might also be helpful for Raman investigations applied in other film systems especially with stress involved.

The authors wish to acknowledge T. Wada in the technical support section and Dr. K. Watanabe for helpful technical support. W.J.Z. would like to thank the Science and Technology Agency (STA) for financial support.

[1] O. Tsuda, Y. Yamada, T. Fujii, and T. Yoshida, J. Vac. Sci. Technol. A **13**, 2843 (1995).
[2] S. Kinder, C. A. Taylor II, and R. Clarke, Appl. Phys. Lett. **64**, 1859 (1994).
[3] D. J. Kester and R. Messier, J. Appl. Phys. **72**, 504 (1992).
[4] M. Sueda, T. Kobayashi, T. Rokkaku, M. Ogawa, T. Watanabe, and S. Morimoto, J. Vac. Sci. Technol. A **16**, 3287 (1998).
[5] H. Hofsäss, C. Ronning, U. Griesmeier, M. Gross, S. Reinke, and M. Kuhr, Appl. Phys. Lett. **67**, 46 (1995).
[6] H. Saitoh and W. Yarbrough, Appl. Phys. Lett. **58**, 2228 (1991).
[7] M. Okamoto, H. Yokoyama, and Y. Osaka, Jpn. J. Appl. Phys., Part 1 **29**, 930 (1990).
[8] W. Dworschak, K. Jung, and H. Ehrhardt, Diamond Relat. Mater. **3**, 337 (1994).
[9] T. Ichiki and T. Yoshida, Appl. Phys. Lett. **64**, 851 (1994).
[10] D. R. McKenzie, W. G. Sainty, and D. Green, Mater. Sci. Forum **54/55**, 193 (1990).
[11] P. B. Mirkarimi, K. F. McCarty, and D. L. Medlin, Mater. Sci. Eng. R. **21**, 47 (1997).
[12] T. Werninghaus, J. Hahn, F. Richter, and D. R. T. Zahn, Appl. Phys. Lett. **70**, 958 (1997).
[13] S. Matsumoto and W. J. Zhang, Jpn. J. Appl. Phys., Part 2 **39**, L442 (2000).
[14] H. Richter, Z. P. Wang, and L. Ley, Solid State Commun. **39**, 635 (1981).
[15] J. Gonzalez-Hernandez, G. H. Azarbayejani, R. Tsu, and F. H. Pollak, Appl. Phys. Lett. **47**, 1350 (1985).
[16] P. Parayanthal and F. H. Pollak, Phys. Rev. Lett. **52**, 1822 (1984).
[17] K. K. Tiong, P. M. Amirtharaj, F. H. Pollak, and D. E. Aspnes, Appl. Phys. Lett. **44**, 122 (1984).
[18] M. Yoshikawa, Y. Mori, M. Maegawa, G. Katagiri, H. Ishida, and A. Ishitani, Appl. Phys. Lett. **62**, 3114 (1993).
[19] H. Herchen and M. A. Cappelli, Phys. Rev. B **47**, 14 193 (1993).
[20] K. Karch, F. Bechstedt, P. Pavone, and D. Strauch, Physica B **219&220**, 445 (1996).
[21] J. A. Sanjurjo, E. López-Cruz, P. Vogl, and M. Cardona, Phys. Rev. B **28**, 4579 (1983).
[22] G. F. Cardinale, D. G. Howitt, K. F. McCarty, D. L. Medlin, P. B. Mirkarimi, and N. R. Moody, Diamond Relat. Mater. **5**, 1295 (1996).
[23] W. J. Zhang, S. Matsumoto, K. Kurashima, and Y. Bando (unpublished).